FERROELECTRIC THIN FILM MICROSTRUCTURE DEVELOPMENT AND RELATED PROPERTY ENHANCEMENT

BRUCE TUTTLE, J.A. VOIGT, T.J. HEADLEY, B.G. POTTER, D. DIMOS, R.W. SCHWARTZ, M.T. DUGGER, J.MICHAEL, R.D. NASBY, T.J. GARINO AND D.C. GOODNOW
Sandia National Laboratories, Albuquerque, New Mexico, USA

Abstract Factors that control phase evolution, microstructural development and ferroelectric domain assemblage are evaluated for chemically prepared lead zirconate titanate (PZT) thin films. Zirconium to titanium stoichiometry is shown to strongly influence microstructure. As Ti content increases, there is an apparent enhancement of the perovskite phase nucleation rate, grain size becomes smaller, and the amount of pyrochlore phase, if present, decreases. While the pyrochlore matrix microstructure for near morphotropic phase boundary composition thin films consists of two interpenetrating nanophases (pyrochlore and an amorphous phase); the pyrochlore microstructure for PZT 20/80 films deposited on MgO substrates is single phase and consists of 10 nm grains. Zirconium to titanium stoichiometry also has a substantial influence on process integration. Near morphotropic phase boundary films exhibit extensive reaction with underlying TiO_2 diffusion barriers; conversely, there is no chemical reaction for identically processed PZT 20/80 thin films. We have attempted to directly correlate the optical quality of PZT thin films to the following microstructural features: 1) presence of a second phase, 2) domain orientation, and 3) nanometer surface morphology.

INTRODUCTION

Control of phase evolution, microstructure, crystallite orientation and ferroelectric domain assemblage is essential for the fabrication of PZT films with optimized electrical and optical properties. Researchers[1,2] have shown that for many, if not all, cases, phase evolution of PZT thin films proceeds from amorphous to pyrochlore to perovskite phases with increasing temperature. Solution chemistry, thermal processing, Pb stoichiometry, Zr to Ti stoichiometry[3] and substrate technology are among the process variables that have been demonstrated to have a substantial impact on PZT phase evolution and film microstructure. Phase assemblage and grain size often impact both electrical and optical properties. Ferroelectric domain assemblage is another factor that substantially influences properties and has been shown to be controlled by the sign of the PZT film stress at the Curie Point.[4] Remanent polarizations ranging from 20 $\mu C/cm^2$ to 60 $\mu C/cm^2$ for single phase perovskite, fine grain PZT thin films, have been measured depending on the stress behavior at the Curie point. The magnitude of the polarization is a major contributor to the pyroelectric, piezeoelectric, and electrooptic figures of merit for PZT thin film devices.

The purpose of this paper is to demonstrate how an array of materials analysis techniques can be used to correlate microstructural and nanostructural features to PZT thin film process integration behavior, electrical characteristics, and optical properties. Among the highlights of this paper are the use of cross-sectional TEM analysis to directly observe heterogeneous perovskite crystal nucleation from an underlying substrate. Another subject discussed in this paper that has not received a great deal of attention is the effect of Zr to Ti stoichiometry on the nanostructure of the intermediary pyrochlore phase. Last, we attempt to correlate the difference in PZT film optical properties of PZT films annealed for different lengths of time to the formation of minor phase surface structures.

EXPERIMENTAL PROCEDURE

The majority of PZT films discussed in this paper were fabricated using a solution chemistry technique termed the inverted mixing order process that has been previously described.[5] The 0.4 M solutions were synthesized by blending the Zr and Ti alkoxide precursors, adding acetic acid and methanol to the solution and then adding the lead (IV) acetate precursor. Additional acetic acid, methanol and distilled water were added to the solution to control the solution viscosity and improve solution stability. Our thin films were deposited by spin coating at 3000 rpm for 30 s. Following deposition, the films were heat treated at 300°C for 5 min on a hot plate. Additional layers were deposited to achieve the desired final film thickness. For 8 layer films (≈800 nm), a crystallization anneal at 650°C was used after deposition of 4 layers.

PZT 53/47, PZT 40/60, PZT 30/70, and PZT 20/80 films were fabricated to determine the effects of Zr to Ti stoichiometry on microstructure and process integration. Film thickness ranged from 200 nm to 800 nm. Rapid thermal processing using a heating rate of 125°C/sec and a soak cycle of 650°C for 10 min was typically used and anneal temperatures from 475°C to 900°C were investigated for PZT 20/80 films. Typical process parameters for furnace annealed films were 650°C for 30 min with a heating rate of 50°C/min. Substrates used in this study included the following: (1) Pt//Ti//SiO_2//Si, (2) MgO, (3) Pt//MgO, and (4) photolithographically defined RuO_2//Ti//TiO_2//SiO_2//Si. The fabrication of highly oriented films was accomplished using high temperature RF magnetron sputtering of Pt onto MgO substrates as described previously.[6]

Proper sample preparation for transmission electron microscopy (TEM) analysis was both a critical and difficult task. Monitoring of the ion milling of cross-sectional samples using an automated laser apparatus was not successful. Cross-sectional samples had to be examined intermittently during milling by TEM to determine if the proper foil thickness had been achieved. Both cross-sectional and plan view specimens were prepared by ion milling with 6 kV argon ions. For cross-sectional views, wafer sections of 6 mm X 6 mm dimensions were epoxied together, mechanically thinned to 100 μm, dimpled to ≈25 μm and then ion milled at an angle of 10° in a liquid nitrogen cold stage. Transmission electron microscopes used in this study included a Philips CM30 AEM operated at 300 kV, a JEOL HEM-2000FX operated at 200 kV, and a HB-501 STEM operated at 100 kV.

Micro X-ray diffraction and backscattered electron Kikuchi pattern (BEKP) analysis have proved useful for characterizing PZT thin film process integration issues. Michael and Goehner[7] have developed a BEKP capability in conjunction with the JSM 6400 scanning electron microscope which allows determination of crystal structure and orientation for "single crystals" as small as 200 nm. For

analysis, the specimen is inclined at an angle between 45° and 80° to the electron beam with the front surface of the YAG scintillator parallel to the beam and between 40 to 60 mm from the specimen. BEKP patterns can be obtained in less than an hour with the newly developed detector system consisting of a YAG scintillator that is fiber optically coupled to a scientific grade thermoelectrically cooled slow scan CCD. Micro-X-ray diffraction was performed with a Rigaku diffractometer with a rotating anode. A Digital Instruments Nanoscope 200 atomic force microscope was used to to determine the surface roughness of both substrates and thin films.

Optical characterization included measurement of refractive indices and electrooptic coefficients parallel and perpendicular to the film plane. A waveguide refractometer technique[8,9] was used to measure these parameters. The technique consists of coupling the light from a He Ne laser into a film by a rutile prism. While the reflected beam intensity is monitored by a Si photodiode, the film / prism arrangement is rotated to change the angle of incidence. Minima in the reflected intensity are observed when waveguiding conditions are met in the film. The sharpness of the reflectivity modes provide a measure of optical quality and the change of the reflectivity minima with applied voltage allows measurement of the electrooptic coefficients.

RESULTS

Control of PZT thin film microstructure, crystallite orientation and domain assemblage by the underlying substrate technology requires that nucleation occurs heterogeneously at the substrate - film interface. Direct evidence for this heterogeneous nucleation is shown in Figure 1. Three perovskite crystals of approximately 40 nm by 25 nm dimension are shown emanating from the underlying (100) MgO surface. The PZT 20/80 film was rapidly thermal processed at 525°C for 15s. SEM micrographs of this film showed that the film contained perovskite crystals, ranging in size from 20 to 500 nm, that were embedded in a fine grain pyrochlore matrix phase. The pyrochlore to perovskite phase transformation proceeds rapidly at this temperature as PZT 20/80 films annealed at 525°C for 90 s were single phase perovskite with ≈1 μm grain size. In our preliminary investigation of this foil, we were able to image 37 of these embryonic perovskite crystals emanating from the substrate // film interface. Detection of these perovskite crystals was greatly facilitated by viewing down the (100) zone axis, for which a strong diffraction contrast is achieved. Epitaxial behavior is observed between substrate and film as previously reported.[5] The perovskite crystal structure of the small crystals was confirmed by electron diffraction. Diffraction spots corresponding to the (100) lattice spacings of the perovskite structure were readily distinguished from the normal face centered cubic MgO pattern.

The zirconium to titanium stoichiometry of PZT thin films has a substantial effect on both phase assemblage and grain size in PZT thin films. Myers and Chapin[10] have shown that while the microstructures of hybrid MOD PZT 75/25 films are diphasic (approximately 50 volume percent perovskite) and consist of large 4 μm perovskite rosettes embedded in a nanometer grain size pyrochlore matrix, identically processed PZT 25/75 films are single phase perovskite with a grain size on the order of 1 μm. We have noted similar microstructural changes with Zr to Ti ratio for films processed using acetate chemistry on photolithographically defined RuO_2 electrodes. While microstructures of crystallized and patterned PZT 53/47 films were diphasic and consisted of 5 μm rosettes embedded in a 50 volume percent pyrochlore matrix, identically

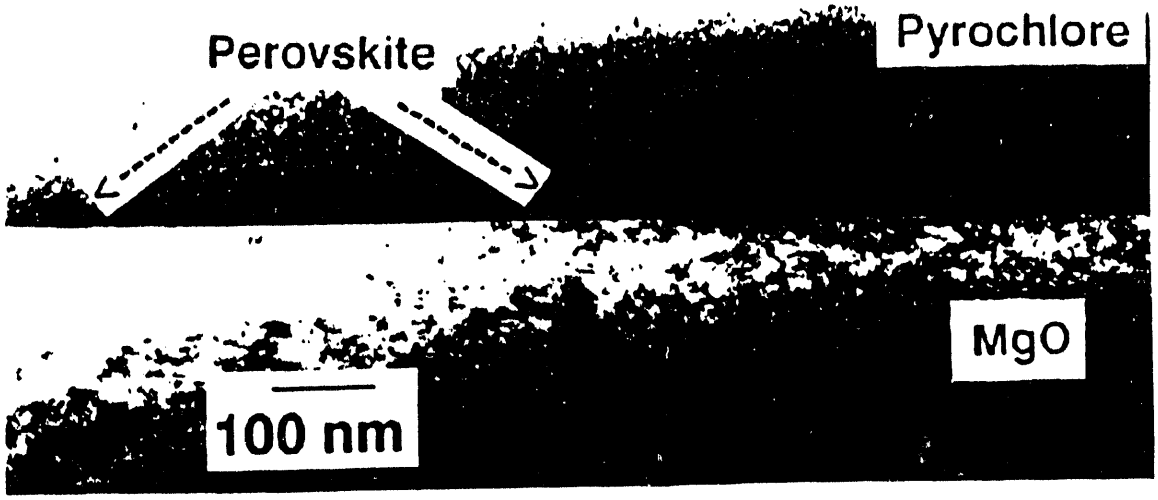

FIGURE 1 Bright field cross-sectional TEM micrograph showing embryonic perovskite crystals at PZT film // MgO substrate interface.

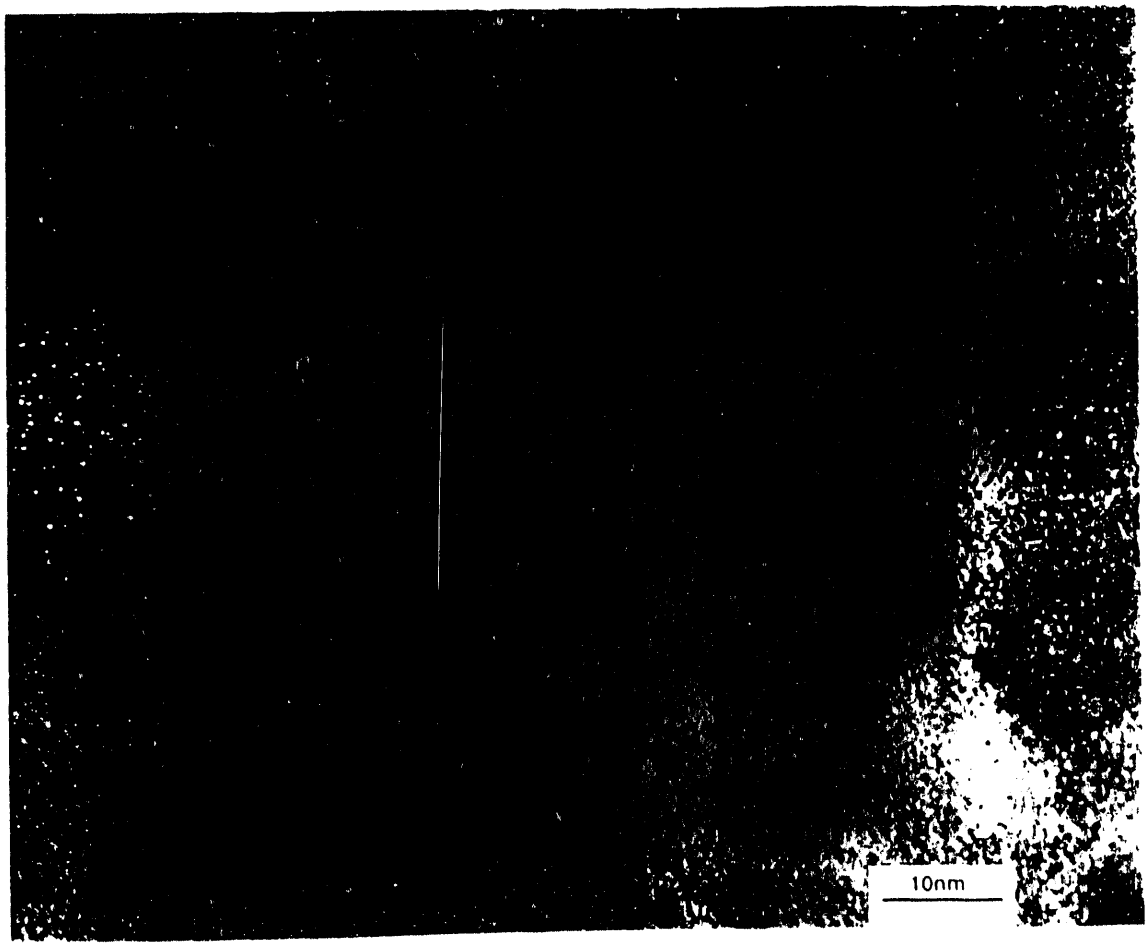

FIGURE 2 Lattice fringe image of pyrochlore phase of PZT 20/80 thin film annealed at 500°C.

processed PZT 30/70 films were essentially single phase perovskite with a grain size of approximately 1 μm. One of the contributing factors to this substantial change in microstructure with Zr to Ti stoichiometry may be the structure of the pyrochlore phase itself. A lattice fringe image of the pyrochlore phase of a PZT 20/80 film annealed at 500°C is shown in Figure 2. While the PZT 20/80 film is single phase pyrochlore consisting of 10 nm grains, the pyrochlore matrix for a similarly processed PZT 53/47 film[1] consists of interpenetrating nanophases of pyrochlore and an amorphous phase of approximately 5 nm spatial dimention. We have determined previously[1] that the amorphous phase is not porosity, but a Pb deficient, Zr rich phase, by interrogating the thinnest sections of the foil using a Vacuum Generators HB-501 STEM (estimated resolution ≈1 nm).

Process integration can depend greatly on the Zr to Ti stoichiometry of PZT thin films. Micrographs of a PZT 40/60 and a PZT 20/80 film that were photolithographically patterned after being dried at 300°C for 5 min are shown in Figure 3. The underlying substrates consist of patterned RuO_2 electrodes that were deposited on a blanket TiO_2 diffusion barrier deposited on SiO_2//Si wafers. The patterned PZT films extend approximately 10 μm past the RuO_2 electrode // TiO_2 interface. After annealing at 675°C, there is significant chemical interaction between the PZT 40/60 film and the underlying TiO_2 diffusion barrier. The interaction region extends 5 μm to 10 μm beyond the original PZT // TiO_2 boundary. Further, the PZT 40/60 microstructure over the RuO_2 electrode is diphasic, consisting of large (3 μm to 10 μm) perovskite rosettes embedded in a fine grain pyrochlore phase that occupies approximately 50 volume percent of the film. In contrast, the interaction for an identically processed PZT 20/80 film is minimal. Further, the PZT 20/80 microstructure over the RuO_2 electrode is almost entirely perovskite in the form of ≈1 μm grains.

The use of EDS, backscattered electron Kikuchi patterns, and micro-X-ray diffraction positively identify various phases in these micron feature size devices. First, BEKP analysis indicates that the 3 μm crystals in the PZT 40/60 film over the RuO_2 electrode are perovksite and that they are randomly oriented. Micro-X-ray diffraction shows that the fine grained matrix is pyrochlore. For the interaction region, which extends beyond the RuO_2//TiO_2 interface, the use of BEKP and EDS analysis determine that some of the larger crystals are perovskite $PbTiO_3$ grains. There is no evidence of Zr diffusion from the film into the interaction region, within the limits of the EDS technique. However, micro-X-ray diffraction analysis indicates that the interfacial region is quite complex, consisting of a mixture of perovskite $PbTiO_3$, cubic pyrochlore ($Pb_2Ti_2O_{7-x}$) and monoclinic $PbTi_3O_7$ phases. The above analyses suggest that Pb from near morphotropic phase boundary composition films preferentially reacts with the TiO_2 buffer layer. This chemical reaction results in inferior device characteristics due to the microstructural changes described above. While we have used PZT films with high Ti content to overcome this problem, another solution to preventing this undesired chemical reaction could be the use of a diffusion barrier other than TiO_2, such as, ZrO_2.

We have demonstrated previously[4] that the sign of film stress at the transformation temperature controls ferroelectric domain orientation. PZT film stress vs. temperature for a PZT film deposited on a platinized MgO substrate is shown in Figure 4. Interestingly, if the film is annealed at 500°C, the film is in planar tension as it cools through the Curie point; whereas, an otherwise identical film processed at 650°C is in planar compression. X-ray diffraction analysis indicates that PZT films deposited directly onto (100) MgO substrates are highly (001) oriented when annealed at 650°C. Conversely, PZT films processed at 500°C are highly (100) oriented. Direct verification of the predominately a-

domain orientation of a PZT 20/80 film deposited directly on MgO and processed at 500°C for 4 min is shown in the bright field TEM micrograph of Figure 5. The film shown contained approximately 50 volume percent perovskite phase in the form of 1 μm cylindrical crystals. Classic relationships between domain structure and crystallography for tetragonally distorted simple perovskite ferroelectrics were confirmed. In the interior of each of the perovskite crystals, a square pattern originating from the diffraction contrast is observed. The sides of the square correspond to the (100) faces of the perovskite crystal. A symmetric pattern of 90° domains are formed in the crystal interior, with the 90° domain walls corresponding to the (110) crystallographic directions. Electron diffraction analysis confirms that 90° a-type domains are formed in the interior of the square as the film cools through the transformation temperature at approximately 450°C. The uniaxial tension at the transformation temperature for this film annealed at 500°C forces the c-axes to be aligned in the plane of the film. The semicircular, in some instances almost triangular, regions of the crystal outside the square area of the crystal consist of alternating c and a domains.

It is well documented[11] for bulk perovskite ferroelectric materials that below a critical grain size, formation of 90° domains is suppressed. The critical grain size for our PZT thin films appears to be on the order of 50 to 150 nm. Previously,[6] we demonstrated that 90° domains existed in PZT thin films of grain size on the order of 2 μm. Further, 90° domains are formed in 0.17 to 0.2 μm diameter perovskite crystals, as shown in Figure 6 for a 300 nm thick PZT 20/80 film. These films were annealed at 475°C for 20 min and contained approximately 80% pyrochlore; thus, the perovskite crystals are embedded in a pyrochlore matrix. We have not observed 90° domain structures for 0.1 μm grain size, 300 nm thick, PZT 40/60 films deposited on Pt coated wafers. While the c/a ratio of the PZT 20/80 films was on the order of 1.042, approximating bulk values, the c/a ratio for a PZT 40/60 film was on the order of 1.015, which is less than the bulk value of 1.025. Our grain size // domain width relationships are different than those observed for bulk ferroelectrics, where Arlt[12] has shown a square root of grain size dependence on domain width for $BaTiO_3$ grains greater than 1 μm. Below 1 μm grain size, domain width decreased far more rapidly with grain size than predicted by square root behavior. Typically, our PZT film domain widths were on the order of 20 to 40 nm, for grain sizes ranging from 0.2 μm to 2 μm. No systematic change in domain width with grain size was observed. The large value of PZT film stress (on the order of 200 MPa compression) and the degree of lattice mismatch (approximately 3%) may in part contribute to the difference from bulk behavior.

We have used the previously described optical waveguide refractometry technique to analyze the optical quality of PZT thin films. Figure 7 is a graph of reflected light intensity as a function of incidence angle for two PZT 40/60 films that were furnace annealed at 650°C for 30 min and 10 min, respectively. The reflectivity minima are substantially broader and less deep in the data for the 30 min film than in the data for the film fired for only 10 min. Qualitatively, a diffuse minimum can imply that a greater amount of optical scattering occurs in the PZT film. In an attempt to determine the cause of this difference between the two films, we have used atomic force microscopy to determine surface roughness. While the rms surface roughness of the 10 min film is 12.7 nm, the surface roughness of the film annealed for 30 min is 6.6 nm. Thus, surface roughness does not appear to be the primary cause of the difference in optical quality of these two films. Further, scanning electron microscopy indicates that both films are single phase perovskite and consist of $\approx$2.0 μm equiaxed grains. X-ray diffraction measurements indicate that both films show a similar degree of highly preferential (001) orientation. Thus, differences in film birefringence due to

crystallite orientation or optical loss due to greater number density of grain boundaries do not appear to be the cause of the difference in optical quality of the two films. Previous work[5] indicates that there is a discontinuous pyrochlore layer (approximately 200 nm thick) on the surface of similar films annealed for 30 min; whereas, films fired for 10 min show no evidence of a second phase layer. Thus, of all the possible origins of optical scattering, the presence of a discontinuous second phase, most likely originating from PbO volatility, appears the most likely cause of enhanced optical scattering in films annealed for 30 min.

Refractive index measurements of PZT films, using the prism coupling technique, provide insight into structure-property relationships. The accuracy of the PZT film index and thickness values, obtained using a computer aided fit to the reflectivity data, critically depends on the optical constants used to describe the other materials in the substrate/film stack. Typically, 3 TE and 2 TM modes were used during fitting to obtain a unique fit to the data. Uncertainty in the fitted extraordinary and ordinary indices of ± 0.003 and ± 0.001, respectively, originate from uncertainties in the experimentally determined Pt optical constants. Previously,[8] refractive indices of 2.544 (n_o) and 2.547 (n_e) were measured for an as crystallized PZT 53/47 film deposited on a platinized Si substrate that was optically well characterized. Applying a field of 125 kV/cm, the birefringence of the film changed from positive to negative, as refractive indices of 2.548 (n_o) and 2.530 (n_e) were measured. For comparison, an as crystallized, highly oriented PZT 40/60 film deposited on platinized MgO had a negative birefringence of -0.009 and refractive indices of 2.584 (n_o) and 2.575 (n_e). Since the highly oriented Pt film on MgO was processed differently than the Pt films on Si, there may be a difference in the optical properties of this Pt film. This difference would influence the PZT film refractive index calculation, which was performed using the optical constants of the Pt films on Si. However, the attainment of negative birefringence in the PZT film processed on MgO is qualitatively in agreement with our premise that compression at the Curie point will cause preferential c-domain alignment. Similarly, the measurement of a positive birefringence for PZT films processed on Si is qualitatively in agreement with the premise that the PZT film is in tension at the Curie point causing preferential a-domain alignment.

SUMMARY

An array of materials analysis techniques were used to correlate microstructural and nanostructural features of PZT thin films to process integration behavior, electrical characteristics, and optical properties. One of the significant findings of this paper was the use of cross-sectional TEM analysis to directly observe heterogeneous PZT perovskite crystal nucleation from an underlying substrate. Quasi-spherical crystals of approximately 40 nm by 25 nm dimension were detected at the MgO interface growing into the pyrochlore phase of a PZT 20/80 film. Also, we determined that there is a substantial difference in the structure of pyrochlore nanophases depending on Zr to Ti stoichiometry. While the PZT 20/80 pyrochlore phase was single phase and consisted of equiaxed 10 nm grains, the structure of a PZT 53/47 pyrochlore phase consisted of two interpenetrating nanophases: pyrochlore and an amorphous phase. An attempt was made to correlate film optical properties to microstructural features. Preliminary results suggest that formation of a lead deficient, discontinuous surface layer is a primary factor in the difference between the waveguide refractometry spectra of PZT 40/60 films annealed for 30 minutes and otherwise identically processed films annealed for 10 min.

ACKNOWLEDGEMENTS

The authors would like to acknowlege the technical support of Mike Eatough, Mary Gonzales, Diana Lamppa, Bonnie McKenzie, and Steve Lockwood. Further, we gratefully acknowledge enlightening technical discussions with Gordon Pike, Angus Kingon, Mike Sinclair, David Clarke, Joe Evans and Jeff Bullington. This work was performed at Sandia National Laboratory supported by the United States Department of Energy under Contract No. DE-ACO4-76-DP00789.

REFERENCES

1. B.A. Tuttle, T.J. Headley, B.C. Bunker, R.W. Schwartz, T.J. Zender, C.L. Hernandez, D.C. Goodnow, R.J. Tissot, and J. Michael, J. Mater. Res., 7, 1876-82 (1992)
2. C. Kwok, S. Desu, and L. Kammerliner, Mater. Res. Soc. Symp. Proc., 200, 83-9 (1990).
3. K.D. Preston and G.H. Haertling, Integrated Ferroelectrics, 1 1, 89-98 (1992).
4. B.A. Tuttle, J.A. Voigt, T.J. Garino, D.C. Goodnow, R.W. Schwartz, D.L. Lamppa, T.J. Headley, and M.O. Eatough, Proc. of the Eighth Int. Symp. on Appl. of Ferroelectrics, edited by M. Liu, A. Safari, A. Kingon and G. Haertling, 344-48 (1992).
5. R.W. Schwartz, B.C. Bunker, D.B. Dimos, R.A. Assink, B.A. Tuttle, D.R. Tallant, and I.A. Weinstock, Proc of 3rd Int. Symp. on Int. Ferroelectrics, 535-46, (1993).
6. B.A. Tuttle, J.A. Voigt, D.C. Goodnow, D.L. Lamppa, T.J. Headley, M.O. Eatough, G. Zender, R.D. Nasby, and S.M. Rodgers, J.Am.Ceram. Soc., 76 1537-44 (1993).
7. J.R. Michael and R.P. Goehner, Microscopy Society of America Bulletin, 23, 168-75 (1993).
8. B.G. Potter, Jr., M.B.Sinclair, and D. Dimos, Appl. Phys. Lett. (Accepted) (1993).
9. S.D. Rammamurthi, S.L. Swartz, J.R. Busch, and V.E. Wood in Ceramic Transactions Vol.25 Ferroelectric Films, (American Ceramic Society, Westerville, OH,) 353-70 (1992).
10. S. A. Myers and L.N. Chappin, Ferroelectric Thin Films (Mater. Res. Soc. Proc., Vol. 200, 231-6 (1990).
11. A.K. Goswami, W.R. Buessem, and L.E. Cross, J.Am.Ceram.Soc., 49, 33-6 (1966).
12. G.Arlt, Ferroelectrics, 104, 217-27 (1990).

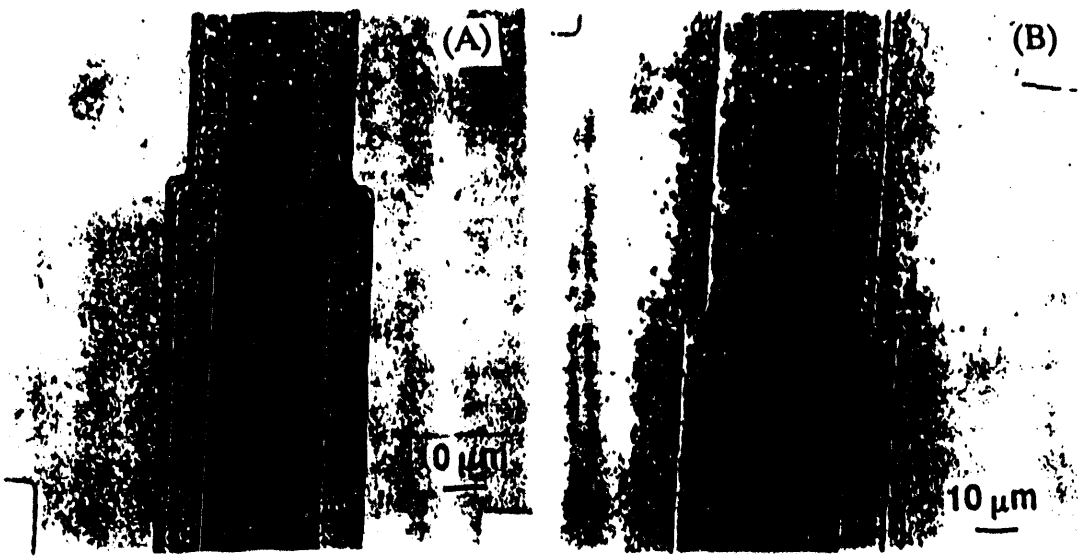

FIGURE 3 Reaction between PZT thin film and underlying TiO_2 diffusion barrier for identically processed films of (A) PZT 20/80 and (B) PZT 40/60.

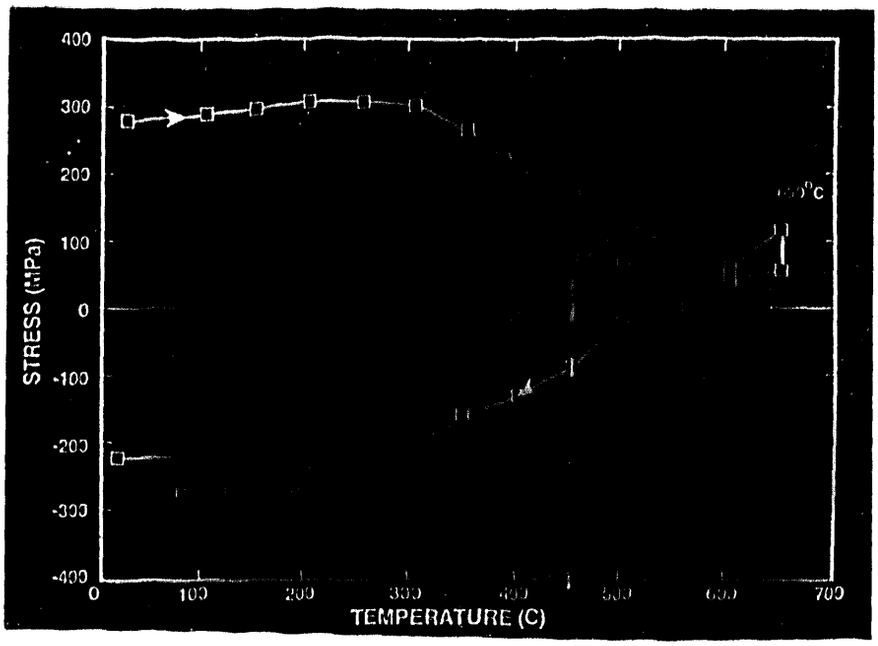

FIGURE 4 PZT film stress versus thermal history for a PZT 53/47 film deposited on a platinum coated (100) MgO substrate.[3]

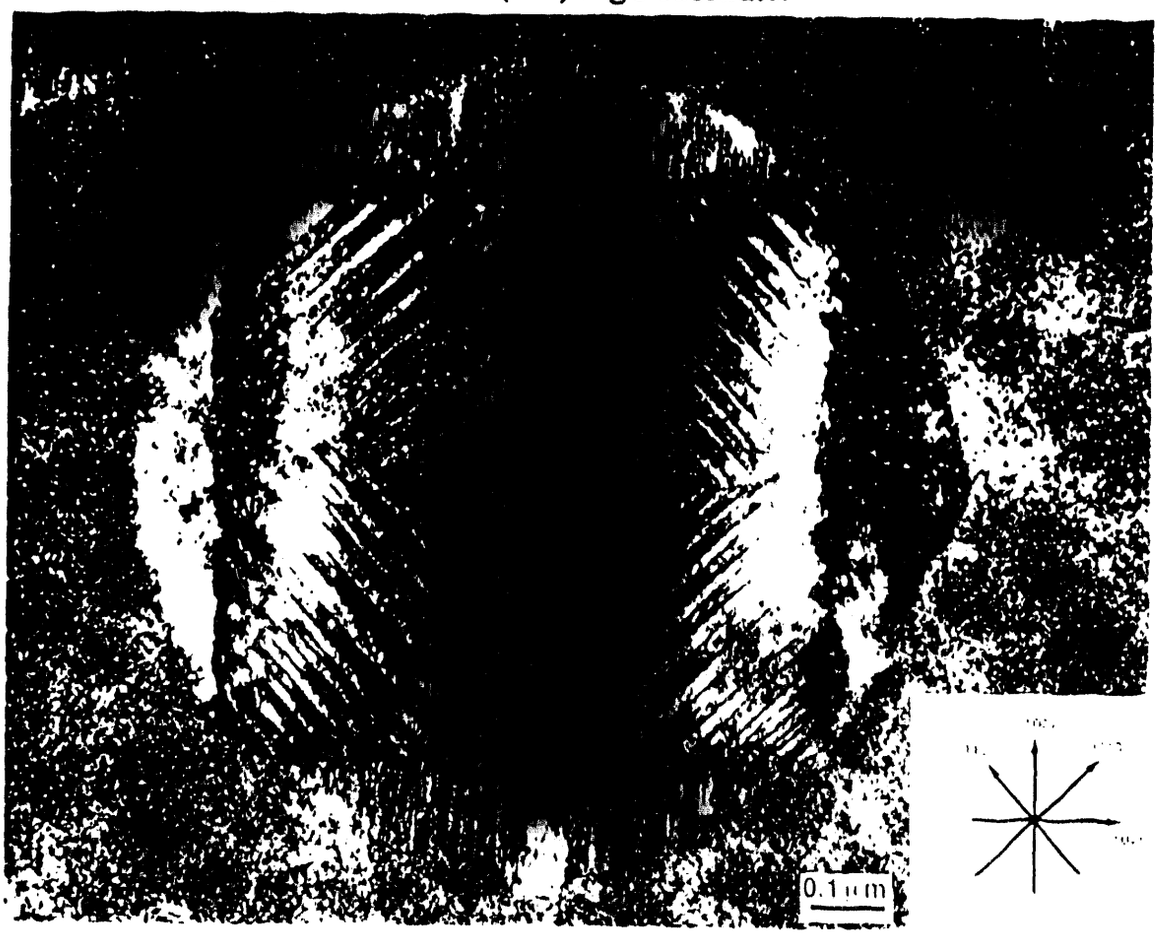

FIGURE 5 Bright field TEM plan view micrograph of perovskite crystal in PZT 20/80 film annealed at 500°C for 4 min.

FIGURE 6 Bright field TEM plan view micrograph of perovskite crystal showing 90° domains in a PZT 20/80 film annealed at 475°C for 20 min.

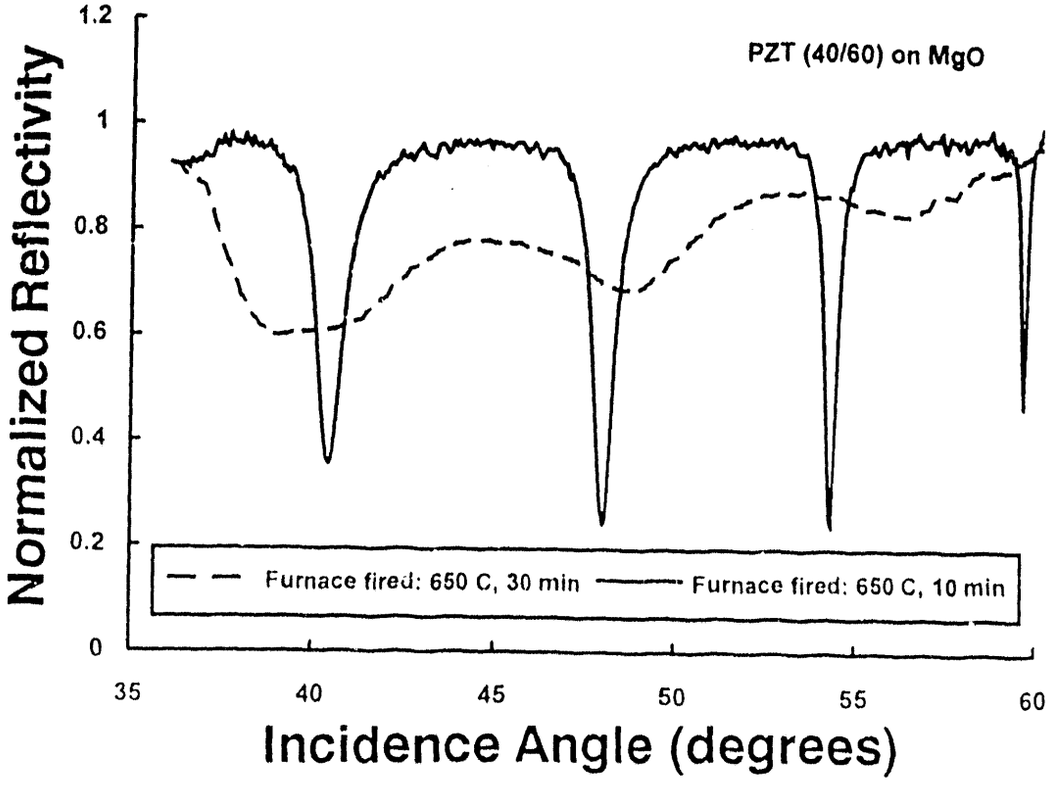

FIGURE 7 Optical waveguide refractometer reflectivity characteristics of two PZT 40/60 films annealed at 650°C for 10 min and 30 min, respectively.

END

DATE
FILMED
12/29/93